

Thermal characterization of soil-cement bricks using mining tailings

<http://dx.doi.org/10.1590/0370-44672021750025>

Ana Cláudia Franca Gomes^{1,4}

<https://orcid.org/0000-0002-2354-8381>

Carol Cardoso Moura Cordeiro^{2,5}

<https://orcid.org/0000-0003-3932-657X>

Ivan Julio Apolonio Callejas^{3,6}

<https://orcid.org/0000-0001-7877-7029>

Sônia Denise Ferreira Rocha^{1,7}

<https://orcid.org/0000-0002-4775-6329>

¹Universidade Federal de Minas Gerais – UFMG, Escola de Engenharia, Departamento de Engenharia de Minas, Belo Horizonte – Minas Gerais - Brasil.

²Universidade Federal de Mato Grosso – UFMT, Faculdade de Engenharia, Cuiabá - Mato Grosso - Brasil.

³Universidade Federal de Mato Grosso – UFMT, Departamento de Arquitetura e Urbanismo, Cuiabá - Mato Grosso - Brasil.

E-mails: ⁴anafrancca@yahoo.com.br, anaclaudiafranccagomes@gmail.com,

⁵carolcardoso.eng@gmail.com,

⁶ivancallejas1973@gmail.com, ⁷sdrocha@demin.ufmg.br

Abstract

Soil-cement bricks are earth construction materials that have been gaining prominence due to their environmental advantages. The Brazilian Technical Standard NBR 8491 establishes physical and mechanical procedures to characterize these bricks. However, the thermal characterization is an important assessment, since it is related to the building's thermal performance. The objective of this study is to thermally characterize a panel of soil-cement bricks produced with mining tailings. For such, its absorptance (α) was evaluated using the ALTA II spectrometer, and its thermal transmittance (U) and thermal resistance (R_T) through the hot box method (ISO 9869). The results enabled the calculation of the thermal capacity (C_T), thermal lag (φ) and solar factor (F_{SO}) of the panel, which were compared to the Brazilian Technical Standards NBR 15575-4 and NBR 15220 for Bioclimatic Zone 8. As a result, the soil-cement body panel showed values of $\alpha = 0.71$, $U = 2.47 \text{ Wm}^{-2}\text{K}^{-1}$, $C_T = 273.4 \text{ kJm}^{-2}\text{K}^{-1}$, $\varphi = 6.02 \text{ h}$ and $F_{SO} = 6.81\%$, meeting the requirements established in the first standard, but failing to attend the second. To comply with the Brazilians specifications, it is suggested to paint bricks with lighter colors focusing on decreasing its absorptance value. Thus, soil-cement bricks may be an environmental alternative to dispose of the waste generated during the mining process, contributing to sustainability.

Keywords: compressed earth blocks, ecological bricks, hot box method, sustainable mining, tailings characterization.

1. Introduction

The civil construction sector is responsible for an environmental setback, in view of its high consumption of natural resources and the emission of pollutants in the stages of material production, execution, and demolition of engineering works. Consequently, construction materials that have sustainable, durable, and less impacting raw materials, such as earth and/or industrial waste, are currently being discussed. In this sense, soil-cement bricks constitute a masonry component composed of a homogeneous, compacted and hardened mixture of soil, Portland

cement, and water, is manufactured with a manual or hydraulic press without the firing process. Assis (2008), Zhang *et al.* (2017) and González-López *et al.* (2018) discuss the advantages of bioconstruction and refer to these bricks as environmentally friendly due to their low emissions of CO₂ and by-products, for being easy to handle, and for not requiring skilled labor.

In Brazil, Technical Standard NBR 8491 (ABNT, 2012) establishes two parameters for consideration in the evaluation of soil-cement bricks: compressive strength and water absorption. How-

ever, building materials are increasingly expected to perform multiple functions. Thus, for Mansour *et al.* (2016), the characterization of soil-cement bricks, in addition to meeting the structural requirements, must also meet the thermal performance parameters, as these are related to the habitability requirements of buildings. Zhang *et al.* (2017) demonstrate that the higher the density of the bricks, the greater their thermal conductivity, although there is no obvious linear relationship between this parameter and the amount of cement added. Mansour *et al.* (2016)

report that this type of unburnt brick presents a bulk density between 1750 to 2100kg m⁻³ and thermal conductivity between 0.75 and 1.3 Wm⁻¹k⁻¹. Fgaier *et al.* (2016) evaluated the thermal capacity of soil-cement bricks that differed from one another in that their materials came from different quarries. It has been shown that the thermal behavior of bricks depends not only on their thickness, but also on the type of soil used.

In this context, NBR 15220 (ABNT, 2005) and NBR 15575 (ABNT, 2013) establish admissible values for thermal parameters, according to Brazilian bioclimatic zones, for construction elements and components as seen in Table 1. Once these are thermally characterized, it is possible to verify if the parameters found are suitable, according to the maximum and minimum values established for each zone. As

such, this article aims to thermally characterize a sealing panel composed of soil-cement bricks, manufactured from cement, soil and mining tailings, from a mining company located in the city of Peixoto de Azevedo (state of Mato Grosso), in the Brazilian Bioclimatic Zone 8 (Z8), see Figure 1. This is the continuation of a study developed by the authors that evaluated the physical and mechanical characteristics of the bricks.

Table 1 - Thermal parameters evaluated according to NBR 15220 and NBR 15575-4.

Parameter evaluated	Standard 15575-4/ Bioclimatic zone		
	Thermal transmittance U (Wm ⁻² K ⁻¹)	1 and 2 $U \leq 2.5$	(If $\alpha \leq 0.6$) 3 - 8 $U \leq 3.7$
Thermal capacity C_T (kJm ⁻² K ⁻¹)	1,2,3,4,5,6 and 7 $C_T \geq 130$	Bioclimatic Zone 8 no requirement	
	Standard 15220-3/ Bioclimatic zone		
Thermal transmittance U (Wm ⁻² K ⁻¹)	1 and 2 $U \leq 3.0$	4, 6 and 7 $U \leq 2.2$	3, 5 and 8 $U \leq 3.6$
Thermal lag φ (h)	$\varphi \leq 4.3$	$\varphi \geq 6.5$	$\varphi \leq 4.3$
Solar factor F_{SO} (%)	$F_{SO} \leq 5.0$	$F_{SO} \leq 3.5$	$F_{SO} \leq 4.0$

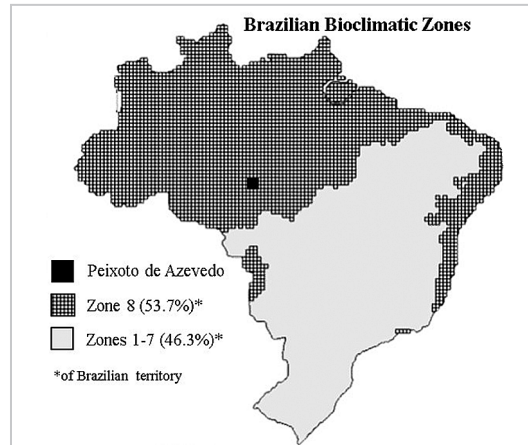


Figure 1 - Brazilian Bioclimatic zone 8 (Z8). Adapted from NBR 15220-3 (ABNT, 2005).

Lima *et al.* (2018) discuss the climatological aspects of the municipality of Peixoto de Azevedo, considering high temperatures, average daily thermal am-

plitude, and long periods of low air humidity. Ferreira *et al.* (2017) concluded that, for Bioclimatic Zone 8, in locations with predominance of hot and dry weather,

such as Peixoto de Azevedo, walls need to have a thermal lag greater than that suggested by the standard ($\varphi \leq 4.3$ h), see Table 1, for greater thermal comfort.

2. Material and methods

The soil-cement bricks were manufactured manually with the aid of molds in the machine MTS-010 (PERMAQ) in Fig. 2a and Fig 2b. The manufacture samples (0.20 m long, 0.10 m wide, and 0.05 m high) -Fig. 2c - were molded with CII-Z-32 cement, mining tailings (silt-clay) and soil (lateritic gravel), both extracted in the city of Peixoto de Azevedo in the Brazilian Bioclimatic Zone

8 (Z8) - Fig. 1. The proportion mixture of 1:5:5 (cement:soil:mining tailings) was defined to provide high bulk density and low void index in the soil-cement brick. The optimum humidity of the mixture (15%) was obtained by the normal Proctor compaction test. The physical and mechanical properties of bricks reached satisfactory bulk density (1800 kg/m⁻³), water absorption (17.9%) and compressive

strength (3.1 MPa), attending the Brazilian standard NBR 8491 (ABNT, 2012). The soil-cement bricks produced were utilized to manufacture a small soil-cement body panel (0.45 m long, 0.10 m wide and 0.45m high) to meet the requirements of the front opening of the thermal chamber where the panel will be tested. A plaster of cement and sand (proportion mixture of 1:8) was used to fix the soil-cement bricks.

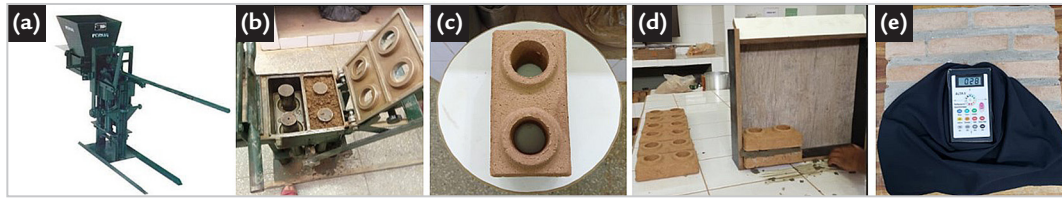


Figure 2 - (a) Equipment used in manufacturing; (b) brick molding (cement, soil and mining tailing); (c) proof body; (d) molding of the soil-cement body panel; (e) the the ALTA II equipment positioned on the wall surface with the dark voltage on the display.

2.1 Thermal chamber - hot box method

The International Standard ISO 9869 (2018) guided the test to determine the soil-cement body panel thermal transmittance, which was carried out simulating an in situ measurement, in a thermal chamber (composed of a metering chamber and a climatic chamber) located in the Laboratory of Technology and Environmental Comfort

of the Federal University of Mato Grosso. The internal dimensions of the metering chamber are 0.65 m long, 0.50 m wide and 0.50 m high, and is made of MDF wood plates and polystyrene plates, aluminum sheets for polystyrene coating, an infrared lamp for the production of heat source inside the chamber (250 W), a Dimmer

device to adjust the intensity of the infrared light, and fans for internal air circulation. The climatic chamber, in turn, has internal dimensions of 0.35 m long, 0.50 m wide and 0.50 m high, and is made of the same materials, serving to isolate the outside of the soil-cement body panel from direct exposure to external climatic conditions.

2.2 Assessment of thermal performance

The aim of the thermal performance characterization was to check if the values found for absorptance (α), thermal transmittance (U), thermal delay (ϕ), thermal

capacity (C_T) and solar factor (F_{SO}) of the soil-cement body panel produced attend the prescribed parameters indicated in technical standards NBR 15575-4 (ABNT, 2013) and

NBR 15220-3 (ABNT, 2005) for Bioclimatic Zone 8, corresponding to the region from which the brick component materials, mining tailing and soil, were extracted.

2.2.1 Absorptance determination test (α)

Due to its availability and very satisfactory precision (Dornelles and Roriz, 2006), the ALTA II spectrometer was used to determine the absorptance (α) of the soil-cement body panel. The equipment provides voltage values (mV) that are converted to reflectance values (ρ). Thus, the reflectance measured by the device refers to the quotient of the radiance rate reflected at the soil-cement body panel by the radiation rate emitted in the spectra of the device. In order for these values to be transformed into reflectance to solar radiation, the methodology of the Brazilian Center for Energy Efficiency in Buildings (CB3E) was adopted. The procedure consists of

placing the ALTA II on the surface of a white sheet of paper (75 g/m²) that will serve as a reference sample for presenting previously known reflectance values (values compared to those of Dornelles and Roriz, 2006).

Reflectance (ρ) is then determined by measurements of eleven different wavelengths (λ), seven of which are in the visible region (between 470 and 700 mV – Blue, Cyan, Green, Yellow, Orange, Red, Deep red) and four of which are in the infrared region (between 735 and 940 mV - IR1, IR2, IR3, IR4). The initial value of the background voltage indicated on the display is previously checked. Then, the equip-

ment is positioned on the surface of the soil-cement body panel, protected with black fabric so as to reduce the interference of ambient light, and five readings are taken for each wavelength (λ). The reflectances were measured in percentage (%) and derived for each wavelength using Equation 1, where ρ_λ is the panel reflectance for a given wavelength (%); V_λ is the sample voltage measured at the wavelength (mV); V_ρ is the sample's dark voltage (mV); $V_{\lambda, ref}$ is the voltage of the reference sample measured at the wavelength (mV); $V_{f, ref}$ is the dark voltage of the reference sample (mV); and ρ_{ref} is the reflectance of the reference sample, already known, in length (%).

$$\rho_\lambda = \left(\frac{V_\lambda - V_f}{V_{\lambda, ref} - V_{f, ref}} \right) \times \rho_{ref} \quad (1)$$

ASTM G173 (2012) describes the procedure for the spectral reflectance values of the sample, ρ_λ , to be converted to the intensities verified in the solar radiation spectrum. First, the spectral reflectance ρ_λ (%) is transformed into a dimensionless value, dividing it by 100.

Then, ρ_λ is multiplied by the global spectral solar radiation at each wavelength (technical standard ASTM G173), which gives the irradiance intensity of the standard solar spectrum that would be reflected by the wall (if the incident source were the sun). This process is

$$G_{(\lambda)reflected} = \rho_\lambda \times G_{(\lambda)} \quad (2)$$

The intensity of the irradiance reflected by the soil-cement body panel was integrated into each of the ALTA II

wavelength intervals (470nm to 940nm) using Equation 3, where $I_{(\lambda \times y)reflected}$ is the global solar radiation intensity reflected by

conducted through Equation 2, where $G_{(\lambda)}$ reflected is the global spectral solar irradiance reflected by the sample ($Wm^{-2}nm^{-1}$); $\rho_{(\lambda)}$ is the spectral reflectance of the (dimensionless) sample and $G_{(\lambda)}$ is the global spectral solar irradiance ($Wm^{-2}nm^{-1}$).

the sample in interval (Wm^{-2}), $G_{(\lambda \times y)reflected}$ is the global solar irradiance reflected by the sample at wavelength λ ($Wm^{-2}nm^{-1}$), $G(\lambda \times y)$

is the global solar irradiance reflected by the sample in wavelength y ($\text{Wm}^{-2}\text{nm}^{-1}$),

λx is wavelength x (nm), and λy is the wavelength y , where $y > x$ (nm).

$$I_{(\lambda x-y)\text{reflected}} = ((G_{(\lambda y)\text{reflected}} + G_{(\lambda x)\text{reflected}} \div 2) \times (\lambda y - \lambda x)) \quad (3)$$

The global solar irradiance was integrated into all λ intervals of the equipment using Equation 4, where $I_{(\lambda x-y)}$ is the

global solar irradiance intensity in interval (Wm^{-2}), $G_{(\lambda x)}$ is the global solar irradiance at wavelength x ($\text{Wm}^{-2}\text{nm}^{-1}$), $G_{(\lambda y)}$ is the

global solar irradiance at wavelength y ($\text{Wm}^{-2}\text{nm}^{-1}$), λx is wavelength x (nm), and λy is wavelength y , where $y > x$ (nm).

$$I_{(\lambda x-y)} = ((G_{(\lambda y)} + G_{(\lambda x)} \div 2) \times (\lambda y - \lambda x)) \quad (4)$$

The solar reflectance adjusted to the standard solar spectrum was calculated using the quotient of the sum of the irradiance intensities reflected by

the sum of the global solar irradiance intensities (Equation 5), where ρ_{solar} is the adjusted solar reflectance (%), $I_{(\lambda x-y)\text{reflected}}$ is the global solar radiance

intensity reflected by the sample in the interval (Wm^{-2}) and $I_{(\lambda x-y)}$ is the global solar radiance intensity in the interval (Wm^{-2}).

$$\rho_{\text{solar}} = \left(\frac{\sum_{\lambda=300}^{\lambda=2500} I_{(\lambda x-y)\text{reflected}}}{\sum_{\lambda=300}^{\lambda=2500} I_{(\lambda x-y)}} \right) \times 100 \quad (5)$$

Finally, with the sum of the parts of reflected and absorbed radiation equal to the total incident radiation,

solar absorptance was calculated from solar reflectance using Equation 6, where α is the (dimensionless) solar

absorption and ρ is the (dimensionless) solar reflectance.

$$\alpha = 1 - \rho \quad (6)$$

2.2.2 Thermal transmittance (U) determination test and error analysis

ISO 9869 (2018) guided the procedures for *in situ* evaluation of the thermal transmittance of the soil-cement body panel, placing it in a protected hot box between the metering chamber and the climatic chamber. The procedures established in Callejas *et al.* (2017) were followed. For this, NTC 10k temperature sensors were installed in the panel for the measurement of the internal surface temperature (T_{si}) and external (T_{se}), in K, and two TMC20HD sensors by Onset-Comp were installed on each face of the soil-cement body panel, facing the inside of the metering chamber and the outside the climate chamber. The sensors were installed centrally and vertically, in a representative area of the soil-cement brick. The two external temperature sensors were positioned between the heat flux sensor (fluxmeter), model HFP01, manufactured by Hukseflux, installed in a vertical position, aiming to measure the heat flux through the test piece. The central idea of the method is to submit a temperature difference (ΔT) between the faces of the wall, generating a heat flux (q), in Wm^{-2} , which will be measured with the fluxmeter. All

sensors were previously calibrated. Their fixation was ensured with adhesive tape, which also prevents direct contact with air. The temperature sensors were then connected to the Onsetcomp automatic data recorder U12-13, and the fluxmeters, which evaluate the heat flux through the panel, were coupled to a tension amplifier and an Onsetcomp U30 automatic data recorder. The climatic chamber was inserted following the installation of all the sensors. Automatic readings (of internal and external temperatures and heat flux rates across the panel) were set for 72 hours, with a sampling interval of 5 minutes. The collected data were entered on a spreadsheet and, through the calculations described below, allowed the determination of thermal parameters.

The soil-cement body panel transmittance was calculated with Equation 7, using the sum of temperatures and heat flux rates across the thickness of the panel over a 72-hour measurement period after steady heat flux was attained. Thus, U_n is the thermal transmittance for each measurement interval ($\text{Wm}^{-2}\text{K}^{-1}$); and j is the time interval of

the measurements during the panel test (5 min). The calculation of U_n for each measurement was done successively, with the calculated value converging asymptotically to the estimated value.

The methodology proposed by Baker (2011) was adopted to estimate the uncertainties in the thermal transmittance value from the uncertainties of the individual measurements of the sensors and the standard deviation (s.d) observed in the test. For measurement uncertainty, the calibration errors of the instruments declared by the manufacturers were assumed. Equation 8 allows the calculation of the general uncertainty about the transmittance estimate (δU_n), where $U_{\text{err}_T_{si}}$, $U_{\text{err}_T_{se}}$ and U_{err_Q} are the values of U calculated by applying the errors during the measurement of the internal temperature, external temperature and heat flux variables, in $\text{Wm}^{-2}\text{K}^{-1}$. In order for the obtained value of U to have a confidence value close to 95%, the coverage factor (k) equal to 2 was adopted. Thus, Equation 9 allows the final calculation of thermal transmittance.

$$U_n = \frac{\sum_{j=1}^n q_j}{\sum_{j=1}^n (T_{sij} - T_{sej})} \quad (7)$$

$$\delta U_n = \sqrt{[(U_n - U_{err_Tsi})^2 + (U_n - U_{err_Tse})^2 + (U_n - U_{errQ})^2 + S.D.^2]} \quad (8)$$

$$U = U_n \pm k. \delta U_n \quad (9)$$

2.2.3 Calculation of thermal resistance (R_T), total thermal capacity (C_T), thermal conductivity (κ), thermal lag (ϕ) and solar factor (F_{SO})

From the calculation of the thermal transmittance (U), it is possible to determine the thermal resistance (R_T in $m^2K W^{-1}$) using Equation 10, according to NBR 15220 (ABNT, 2005).

Specific heat (c in $J kg^{-1} K^{-1}$) was estimated by Equation 11 - NBR 15220 (ABNT, 2005) - where ρ is the specific mass of the material ($kg m^{-3}$); e is the soil-cement body panel thickness (m); A is the panel area (m^2); q_1 and q_2 are the internal and external average heat fluxes, respectively (W); i is the representation of each

measurement; Δt is the time variation between each measurement (s), T_1 and T_2 are the average of the internal (T_{si}) and external (T_{se}) temperatures, respectively ($^{\circ}C$); and T_i is the initial temperature, associated with the ambient temperature at the beginning of the measurements ($^{\circ}C$).

The thermal conductivity (κ) in $W(m.K)^{-1}$ was estimated as proposed by Nicolau, Güths and Silva (2002) using Equation 12.

Total thermal capacity (C_T), on the other hand, was calculated using the

contribution of each element present in the structure of the soil-cement body panel through Equation 13 - NBR 15220 (ABNT, 2005).

The thermal lag (ϕ), in hours, was determined in accordance with the recommendation of NBR 15220 (ABNT, 2005) using Equation 14.

Finally, the solar factor (F_{SO}) was calculated through Equation 15 - NBR 15220 (ABNT, 2005), where U is the total thermal transmittance of the wall and α is the absorptance of the wall.

$$R_T = 1/U_T \quad (10)$$

$$c = \frac{1}{\rho e A} (\sum_{i=1}^n q_1 - \sum_{i=1}^n q_2) \cdot \Delta t / \frac{(T_1 + T_2)}{2} - T_i \quad (11)$$

$$\kappa = \frac{1}{2} (q_1 + q_2) \frac{e}{A \cdot (T_1 + T_2)} \quad (12)$$

$$C_T = \sum_{n=1}^n k. R. c. \rho = \sum_{n=1}^n e. c. \rho \quad (13)$$

$$\phi = 0.7284 \sqrt{R_t \cdot C_T} \quad (14)$$

$$FS = 4 \cdot U \cdot \alpha \quad (15)$$

3. Results and discussions

The reflectance (ρ) and absorptance (α) indices of the soil-cement body panel, constructed with soil-cement bricks, were determined by calculations made from the reflected

irradiance readings, obtained using the ALTA II spectrometer. Table 2 contains the wavelengths (λ) analyzed, the reference ρ values of the sheet of paper characterized by Dornelles and

Roriz (2006) and the ρ values of the panel. Figure 2e illustrates the ALTA II equipment positioned on the wall surface with the dark voltage on the display.

Table 2 - Reflections obtained for the soil-cement body panel.

ALTA II	Wavelength in the visible region							Wavelength in the infrared region			
	Color	Blue	Cyan	Green	Yellow	Orange	Red	Deep Red	IR1	IR2	IR3
λ (nm)	470	525	560	585	600	645	700	735	810	880	940
ρ ref (%)*	87.8	84.2	80.7	79.8	79.7	87.7	95.1	96.6	96.8	97.3	95.8
ρ panel (%)	12.1	15.6	15.8	14.9	16.6	20.0	22.9	25.4	25.9	24.3	22.4

* Values characterized by Dornelles e Roriz (2006).

The soil-cement body panel presented reflectance (ρ) of 28.5% and, consequently,

absorptance (α) of 71.5%. Standard NBR 15220-3 (ABNT, 2012) estimates α values

of 30-75% for shades between yellow and red, 70-80% for red ceramic brick and clay

tiles, and 65-80% for exposed bricks. It is observed that, although the absorptance value found for the panel of soil-cement bricks is between these intervals, the Brazilian technical standard is not specific for this type of material.

Through the protected hot box, internal and external temperatures and heat

fluxes were taken every 5 minutes for 72 hours, totaling 865 measurements. Figure 3 illustrates the soil-cement body panel positioned in front of the metering chamber, the closed climate chamber, and photos taken with a FLIR thermographic camera, which performs instant surface temperature reading. The data captured during the conduc-

tion of the test enabled the making of the graph in Figure 4. It is noted that, in the first 24 hours, there was a period of oscillation in the temperatures, until the stationary period was reached, when the stabilization of both the internal and external temperatures was checked. A similar behavior was observed for thermal transmittance.



Figure 3 - (a) the panel with fluxmeter and temperature sensors, (b) assembled climate chamber and (c) photo of the panel obtained with the FLIR thermal imager after 72 hours of testing.

Then, for the calculations, the average for 288 records were considered, equivalent to the last 24 hours of measurement. The average external surface temperature (T_{se}) was 44.00°C and the average internal surface temperature (T_{si}) was 61.02°C. The average value between the temperature differences between the internal and external faces was approximately 15.08°C, while the average heat flux through the panel was 68.45 Wm⁻². Through these values,

the thermal transmittance was calculated for each measurement interval (U_n), and it can be observed that they converged asymptotically to a value close to the true value after the 24-hour period, as expected (Figure 4). Thus, the hot box method enabled the average value of U_n and the statistical uncertainty of the measurement of 4.00 ± 0.06 Wm⁻²K⁻¹ to be obtained, which delimits the confidence interval of the test at

$3.94 \leq U_n \leq 4.06$ Wm⁻²K⁻¹; while the thermal resistance was m²KW⁻¹ with a confidence interval between $0.20 \leq R \leq 0.30$ m²KW⁻¹. The total average thermal resistance (R_t) of 0.41 m²KW⁻¹ was calculated by adding the average of the thermal resistance with the internal and external thermal resistances of the air. Thus, the total average thermal transmittance (U) was calculated by the inverse of R_t , resulting in 2.47 Wm⁻²K⁻¹.

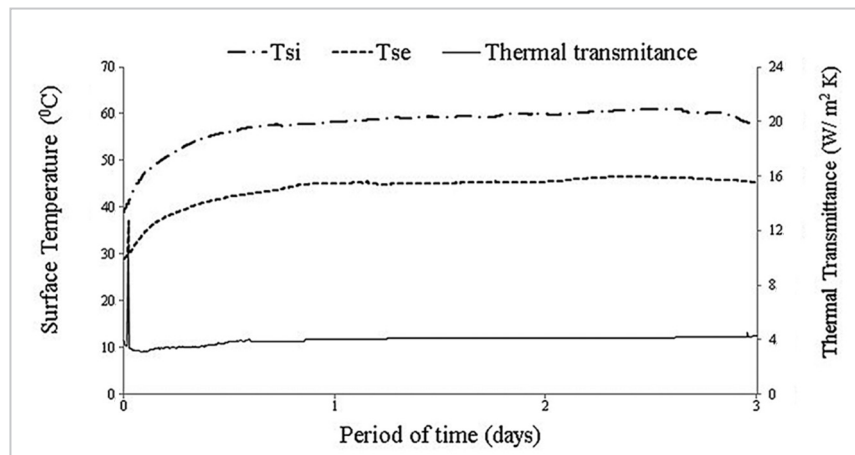


Figure 4 - Internal and external wall temperature and thermal transmittance obtained during the test.

The thermal conductivity (κ) of the material (Equation 12) was equivalent to 0.86 W(m.K)⁻¹. Consulting NBR 15220-2 (ABNT, 2005), this parameter was verified for bricks and clay tiles (κ between 0.70 - 1.05W(m.K)⁻¹), and for materials with clay and sandy characteristics (κ between 0.52 - 0.93W(m.K)⁻¹), since the brick was produced with tailings (silt-clay) and soil (lateritic gravel). Mansour *et al.* (2016) report that this type of unfired brick has a bulk density between 1750 to 2100kg m⁻³ and ther-

mal conductivity between 0.75 and 1.3 Wm⁻¹k⁻¹. As discussed for absorptance, although the thermal conductivity value (κ) found for the soil-cement body panel is among these intervals, the Brazilian technical standard is not specific for this type of material.

Mansour *et al.* (2016) demonstrated that the compaction pressure in the manufacture of soil-cement bricks importantly influences their bulk density, which, in turn, directly impacts their thermal and mechanical properties. In

general, the greater the pressure in the manufacture of the bricks, the greater the compressive strength (f_t) and the thermal conductivity (k) of the bricks will be. As an example, the authors obtained bricks with a bulk density of 1900kgm⁻³ with compressive strength of 2.8MPa and $\kappa = 1.00$ Wm⁻¹.K⁻¹; for bricks with a bulk density of 1750kgm⁻³ the f_t was 1.0MPa and $\kappa = 0.75$ Wm⁻¹.K⁻¹ (produced with the same material). Thus, the bricks evaluated (mixture 1: 5: 5), with a bulk density of 1800kgm⁻³ (calculated

by dividing the mass of dry bricks by their volume), have the potential to reach higher values of bulk density and compressive strength with the increase of the pressing pressure in its manufacture. However, its thermal conductivity would also be higher.

The data of thermal transmittance (U) and thermal capacity (C_T) obtained was $2.47 \text{ Wm}^{-2}\text{K}^{-1}$ and $273.4 \text{ kJm}^{-2}\text{K}^{-1}$, respectively. These values were compared to those established by NBR 15575-4 (ABNT, 2013) – Table 1 - for Brazilian climatic zones. The panel was built with soil-cement bricks made of mining tailings and soil collected from Z8. It is observed that it meets the requirement for thermal transmittance (U), not only for Bioclimatic Zone 8, but for all the others. Regarding thermal capacity (C_T), the standard does not present requirements for this parameter in Z8, although it corresponds to almost 54% of the entire Brazilian territory (Fig. 1). However, the C_T value found ($273.4 \text{ kJm}^{-2}\text{K}^{-1}$) is higher than the required value ($130 \text{ kJm}^{-2}\text{K}^{-1}$) for zones 1 – 7, in accordance with this standard. As such, a greater amount of heat would be necessary for the temperature of the soil-cement brick to change by 1°C in these regions.

The value obtained for U also respects the limit stipulated by NBR 15220-3 (ABNT, 2005) – Table 1 - for the Brazilian Bioclimatic Zone 8. According to this standard, the value found for solar factor ($F_{50} = 6.81\%$) - Equation 15 - did not meet the value stipulated for Z8 ($F_{50} \leq 4.0$).

4. Conclusions

The thermal absorptance characterization of the soil-cement body panel indicated a high value for this property ($\alpha = 0.71$). However, the brick color can be changed to lighter tones, increasing its reflectance (ρ) and decreasing its α , thus placing its solar factor (F_{50}) within the standardized limits. The test in the thermal box indicated values compatible with the ceramic bricks traditionally used to build a conventional vertical panel system in Brazil. However, the apparent thermal conductivity ($\kappa = 0.86 \text{ Wm}^{-1}\text{K}^{-1}$)

However, this parameter is directly proportional to thermal transmittance (U) and absorptance (α). Thus, simply painting the bricks, which has brown shades (between yellow and red), a light color (with $\alpha < 0.3$) would reduce the F_{50} value, therefore conforming to the technical standard (Dornelles and Roriz, 2006).

NBR 15220-3 (ABNT, 2005) also suggests that lower values of thermal transmittance can be achieved by adding a mortar coating on the external face, the internal face, or both, with a composition of the same thermal conductivity (the same mixture of tailings and soil), in order to maintain compatibility between the components of the vertical sealing system. This proposal, in addition to causing a lower solar factor value, also generates a greater tailings destination.

The thermal lag obtained ($\varphi = 6.02\text{h}$) did not meet NBR 15220-3 (ABNT, 2005) – Table 1 - since it exceeded the maximum value allowed ($\varphi \leq 4.3$) for Z8, which indicates that a longer time would be needed for the temperature variation in the outside to be recorded in the inside of a building. According to this standard, for Z8, the thermal lag established (φ) has the city of Manaus as reference, where temperatures are high, but the thermal amplitude is low. In these cases, no major thermal lags are indicated, since this is attained through thermal mass (thick walls with high thermal capacities). However, Ferreira *et al.* (2017) concluded that, for Z8, in locations

was lower than that of ceramic bricks with densities similar to that of the presently studied brick ($\kappa = 1.05 \text{ Wm}^{-1}\text{K}^{-1}$). Therefore, from a thermal point of view, soil-cement bricks with tailings have the potential to replace the traditional ceramic bricks commonly used in vertical panel systems, according to the necessary adaptation for each Brazilian bioclimatic zone. The value found for thermal transmittance U ($2.47 \text{ Wm}^{-2}\text{K}^{-1}$) is in accordance with those estimated by NBR 15575-4 and NBR 15220, and the solar factor

with predominance of hot and dry weather, such as the city of Peixoto de Azevedo [Lima *et al.* (2018)], walls need to have a thermal lag greater than that suggested by the standard ($\varphi \leq 4.3\text{h}$), for greater thermal comfort.

For the thermal lag to be in conformity with the other bioclimatic zones in which $\varphi \geq 6.5 \text{ h}$ – Table 1, it is necessary to increase the thermal resistance of the soil-cement body panel (Eq. 14). Thermal resistance can be increased by adding a layer of mortar coating, as recommended by NBR 15220-3 (ABNT, 2005). Moreover, Mansour *et al.* (2016) demonstrated that the pressing pressure of the soil-cement brick has a direct influence on its bulk density, which impacts its mechanical and thermal behavior. In general, the higher the pressing pressure, the greater the compressive strength of the brick; however, the lower its thermal resistance. This is because greater pressing promotes a greater packaging of the grains present in the mixture, decreasing its porosity. The pores, in turn, help in the non-propagation of heat from one surface to another, increasing the thermal resistance of the material. Since compressive strength is one of the most important parameters to classify a brick as soil-cement type, it would be more interesting to increase the e thickness of the bricks, since Fgaier *et al.* (2016) demonstrated that thermal resistance increases linearly with brick thickness. Thus, as seen from Eq. 13, a larger e implies a larger C_T , which, in turn, increases the value of the thermal lag.

found ($F_{50} = 6.81$) is nonconforming with the maximum recommended ($F_{50} \leq 4.0$). It is observed that these standards are not specific for soil-cement bricks and do not present requirements for thermal capacity (C_T) in the Brazilian Bioclimatic zone 8.

Based on the technical characteristics of the soil-cement bricks determined in this research, it is possible to state that it is an environmental alternative to dispose of the waste generated during the mining process, contributing to sustainability.

Acknowledgements

The authors acknowledge CNPq, CAPES, DEMIN/ UFMG, PPGEM/

UFMG, FAENG/UFMT, FAET/UFMT, and Borges Construtora com-

pany for the support on conduction of experiments

References

- AMERICAN SOCIETY FOR TESTING AND MATERIALS. *ASTM G173-03*: Standard tables for reference solar spectral irradiances: direct normal and hemispherical on 37° tilted surface. West Conshohoken, PA: ASTM International, 2012.
- ASSIS, J. B. S. *Determinação experimental da resistência à tração na flexão em paredes construídas com blocos encaixáveis de solo-cimento*. 2008. Tese (Doutorado em Engenharia de Estruturas) – Escola de Engenharia, Universidade Federal de Minas Gerais, Belo Horizonte, 2008.
- ASSOCIAÇÃO BRASILEIRA DE NORMAS TÉCNICAS. *ABNT NBR 15220-1*: Desempenho térmico de edificações Parte 1: Definições, símbolos e unidades. Rio de Janeiro: ABNT, 2005.
- ASSOCIAÇÃO BRASILEIRA DE NORMAS TÉCNICAS. *ABNT NBR 15220-2*: Desempenho térmico de edificações Parte 2: Método de célula da transmitância térmica, da capacidade térmica, do atraso térmico e do fator solar de elementos e componentes de edificações. Rio de Janeiro: ABNT, 2005.
- ASSOCIAÇÃO BRASILEIRA DE NORMAS TÉCNICAS. *ABNT NBR 15220-3*: Desempenho térmico de edificações Parte 3: Zoneamento bioclimático brasileiro e diretrizes construtivas para habitações unifamiliares de interesse social. Rio de Janeiro: ABNT, 2005.
- ASSOCIAÇÃO BRASILEIRA DE NORMAS TÉCNICAS. *ABNT NBR 15220-4*: Desempenho térmico de edificações Parte 4: Medição da resistência térmica e da condutividade térmica pelo princípio da placa quente protegida. Rio de Janeiro: ABNT, 2005.
- ASSOCIAÇÃO BRASILEIRA DE NORMAS TÉCNICAS. *ABNT NBR 8491*: Tijolo de solo-cimento: requisitos. Rio de Janeiro: ABNT, 2012.
- ASSOCIAÇÃO BRASILEIRA DE NORMAS TÉCNICAS. *ABNT NBR 15575-1*: Edificações habitacionais – Desempenho. Parte 1: Requisitos gerais. Rio de Janeiro: ABNT, 2013.
- ASSOCIAÇÃO BRASILEIRA DE NORMAS TÉCNICAS. *ABNT NBR 15575-4*: Edificações habitacionais – Desempenho. Parte 4: Requisitos para os sistemas de vedações verticais internas e externas - SVVIE. Rio de Janeiro: ABNT, 2013.
- BAKER, P. *U-values and traditional buildings: In situ measurements and their comparisons to calculated values*. Scotland: Glasgow Caledonian University, 2011.70p. (Technical Paper 10).
- CALLEJAS, I.J.A.; DURANTE, L. C.; OLIVEIRA, A. S. Thermal resistance and conductivity of recycled construction and demolition waste (RCDW) concrete blocks. *REM – International Engineering Journal*, v. 70, n. 2, p. 167-173, 2017.
- DORNELLES, K. A.; RORIZ, M. A Method to identify the solar absorptance of opaque surfaces with a low-cost spectrometer. *In: INTERNATIONAL CONFERENCE ON PASSIVE AND LOW ENERGY ARCHITECTURE*, 23., 2006, Geneva. *Proceedings [...]*. Geneva: PLEA, 2006.
- EL FGAIER, F.; LAFHAJ, Z.; ANTCZAK, E.; CHAPISEAU, C. Dynamic thermal performance of three types of unfired earth bricks. *Applied Thermal Engineering*, v.93, p.377-383, 2016.
- FERREIRA, C. C.; SOUZA, H. A.; ASSIS, E. S. Discussion of the limits of the thermal properties of building envelopes according to Brazilian thermal performance standards. *Ambiente Construído*. v.17, n.1, p. 183 – 200, 2017.
- GONZÁLEZ-LÓPEZ, J. R.; ALVARADO, C. A. J.; FRANCIS, B. A.; RANGEL, J. M. M. Compaction effect on the compressive strength and durability of stabilized earth blocks. *Construction and Building Materials*, v. 163, p.179-188, 2018.
- INTERNATIONAL ORGANIZATION FOR STANDARDIZATION. *ISO 9869*: Thermal insulation - Building elements – In-situ measurement of thermal resistance and thermal transmittance. Geneva: ISO, 1994.
- LIMA, E. B. N. R.; MODESTO, P. F.; MOURA, R. M. P. (org.). *Plano municipal de saneamento básico: Peixoto de Azevedo-MT*. Cuiabá: EdUFMT, 2018. p. 67-68.
- MANSOUR, M. B.; JELIDI, A.; CHERIF, A. S.; JABRALLAH, S. B. Optimizing thermal and mechanical performance of compressed earth blocks (CEB). *Construction and Building Materials*, v. 104, p. 44-51, 2016.
- NICOLAU, V. P.; GÜTHS, S.; SILVA, M. G. Thermal conductivity and specific heat measurement of low conductivity materials using heat flux meters, *In: EUROPEAN CONFERENCE ON THERMOPHYSICAL PROPERTIES*, 16., 2002, London. *Proceedings [...]*. London: ECTP, 2002.
- ZHANG, L.; GUSTAVSEN, A.; JELLE, B. P.; YANG, L.; GAO, T.; WANG, Y. Thermal conductivity of cement stabilized earth blocks. *Construction and Building Materials*, v. 151, p. 504-511, 2017.

Received: 19 April 2021 - Accepted: 24 November 2021.



All content of the journal, except where identified, is licensed under a Creative Commons attribution-type BY.